

UCRL--93262

DE86 007154

HIGH GAIN AND HIGH EXTRACTION EFFICIENCY
FROM A FREE ELECTRON LASER AMPLIFIER
OPERATING IN THE MILLIMETER WAVE REGIME

T. J. Orzechowski, B. R. Anderson,
W. M. Fawley, D. Prosnitz, E. T. Scharlemann,
S. M. Yarema, A. M. Sessler, D. B. Hopkins,
A. C. Paul, J. S. Wurtele

SEVENTH INTERNATIONAL FREE ELECTRON LASER
CONFERENCE

Tahoe City, California
September 8-13, 1985

October 1, 1985

The logo for Lawrence Livermore National Laboratory is a large, stylized 'V' shape. The top horizontal bar of the 'V' is white. The two slanted sides of the 'V' are filled with a black and white stippled pattern. The text 'Lawrence Livermore National Laboratory' is written in a sans-serif font, oriented vertically along the right-hand slanted side of the 'V'.

Lawrence
Livermore
National
Laboratory

This is a preprint of a paper intended for publication in a journal or proceedings. Since changes may be made before publication, this preprint is made available with the understanding that it will not be cited or reproduced without the permission of the author.

DISTRIBUTION OF THIS DOCUMENT IS UNLIMITED

HIGH GAIN AND HIGH EXTRACTION EFFICIENCY FROM A
FREE ELECTRON LASER AMPLIFIER OPERATING IN THE MILLIMETER WAVE REGIME

T. J. Orzechowski, B. R. Anderson[†], W. M. Fawley, D. Frosnitz,
E. T. Scharlemann, S. M. Yarema
Lawrence Livermore National Laboratory*
Livermore, California 94550

A. M. Sessler, D. B. Hopkins, A. C. Paul, J. S. Wurtele^{††}
Lawrence Berkeley Laboratory**
Berkeley, California 94720

October 1, 1985

ABSTRACT

Experiments at the Electron Laser Facility have generated peak microwave power of 180 MW at 35 GHz. The facility is operated as a single pass amplifier. Gain in excess of 30 dB/m has been observed up to saturation of the amplifier. For the 3 MeV, 850 Amp electron beam, the radiation corresponds to 7% energy extraction from the electron beam. Beyond saturation, the electron beam output power exhibits oscillations corresponding to the synchrotron

MASTER

*Performed jointly under the auspices of the U. S. Department of Energy by Lawrence Livermore National Laboratory under W-7405-ENG-48 and for the Department of Defense under SDIO/BMD-ATC MIPR No. W3-RPD-53-A127.

**This work was supported by the Director, Advanced Energy Systems, Basic Energy Sciences, Office of Energy Research, U. S. Department of Energy under Contract No. DE-AC03-76SF00098.

[†]Present address: Air Force Weapons Laboratory/Kirtland AFB, Albuquerque, NM 87117

^{††}Present address: Plasma Fusion Center, Massachusetts Institute of Technology, Cambridge, MA 02139

DISTRIBUTION OF THIS DOCUMENT IS UNLIMITED

2500

motion of the trapped electrons in the ponderomotive well. In addition, the TE_{21} and TM_{21} modes have been studied and have power levels comparable to the fundamental. Third harmonic (105 GHz) radiation has been measured at power levels on the order of a few percent of the peak fundamental power.

INTRODUCTION

The Electron Laser Facility (ELF) is a Free Electron Laser amplifier operating in the millimeter wave regime. ELF uses the electron beam produced by the Experimental Test Accelerator (ETA) which is a linear induction accelerator. Both ELF and ETA have been described in previous publications and will be briefly reviewed here.¹ The experimental results discussed here include small signal gain, exponential gain in the amplifier mode, saturation of the amplifier and the effects of synchrotron motion beyond saturation. Higher order modes and third harmonic radiation have been studied in the amplifier mode of operation.

DESCRIPTION OF EXPERIMENT

Present experiments on ELF use a 3 MeV, 850 Amp beam generated by ETA. The gun in ETA has been modified to use a field emission cathode² yielding a peak current of 3 kA. An emittance filter³ in the ETA/ELF beamline is used to reduce the current and emittance of the beam injected into the wiggler. The brightness of the electron beam is 2×10^4 A/cm²-rad², which is a factor of two higher than the electron beam formed with a flashboard cathode and used in the preliminary ELF experiments.⁴ The pulse length of the electron beam

through the wiggler is 12 to 15 nsec long. Although ETA is capable of operating at 1 pps, the experiment is run at 1/2 Hz to reduce the average power load on the wiggler.

The linearly polarized, pulsed electromagnetic wiggler is 3-meters long with a period of 9.8 cm.⁵ In addition, each two periods of the wiggler is independently controlled. We used this feature to vary both the amplitude and the length of the wiggler magnetic field. When the wiggler length was varied, the section of wiggler not used for FEL resonance was set at 40% of the wiggler field in the resonant section. This reduced field assisted in guiding the electron beam out of the interaction region but did not contribute to the FEL interaction. Horizontal stabilization is provided by continuous (horizontal) focusing quadrupoles.

The input signal to the FEL amplifier was provided by a 100 kW, 35 GHz magnetron with a pulse length of 500 nsec. The magnetron is matched to the oversized waveguide of the interaction region (3 cm x 10 cm) using gradual waveguide tapers. The FEL is matched to the TE_{01} mode of the oversized waveguide: the wiggler plane (and therefore the electric field) is parallel to the wide dimension of the waveguide. The magnetron is transit time isolated ($L/c > 15$ nsec) from the interaction region in order to ensure single pass performance of the amplifier. The input signal is reflected into the interaction region by a fine mesh screen that is virtually transparent to the electron beam. The electron beam is injected through the screen into the interaction region.

When the small signal gain of the system is measured the magnetron is replaced with a detector station using bandpass filters, variable attenuators, and a crystal detector. A movable microwave short is inserted into the inter-

action region⁴. As this short is extracted from the interaction region, the effective interaction region is lengthened. Any microwave signal generated in this region reflects off the short and is monitored at the detector station. Both the small signal gain technique and the normal amplifier mode of operation are illustrated in Fig. 1.

SMALL SIGNAL GAIN

The results of the small signal gain measurement are shown in Fig. 2. The detector system includes a low pass and band pass filter (33.8-35.2 GHz) to ensure that the signal being measured is in the resonant frequency bandwidth (the wiggler field is set to a value corresponding to resonance at 34.6 GHz). Also, the detector system is in fundamental guide (K_a -band, WR28) and the smooth tapers are used to guide the microwaves from the over-sized guide to the fundamental. Therefore, any higher order modes excited in the interaction region are beyond cutoff in the fundamental guide and the small signal gain only measures the gain in the fundamental mode. The small signal gain is 26.6 dB/m through the wiggler. The radiation grows from an effective input signal of 1.5 mW. This small signal gain is approximately twice the gain measured previously⁴ where we had half the input current but same emittance.

AMPLIFIER EXPERIMENTS

In the amplifier mode, the detector station is replaced by the magnetron operating at 34.6 GHz with an output power of 100 kW and pulse length of

500 nsec. We lose 3 dB of the input signal in tapering from the fundamental oversized guide and reflecting off two mitre bends into the interaction region. Therefore, 50 kW enters the interaction region.

Crystal detectors are used to monitor the amplified radiation. The interaction guide tapers to a standard WR229 waveguide beyond the wiggler. The WR229 guide is terminated in a large (8' long x 4' diameter) vacuum tank ($P \sim 10^{-5}T$) the walls of which are lined with a microwave absorbing material. The amplified signal radiates into one end of the tank and is received in a fundamental guide on the far side of the tank. The diffraction loss results in 41 dB of attenuation. Directional couplers (one under vacuum) and precision variable attenuators are used to attenuate the signal further down to the milliwatt regime where the crystal detectors operate. The attenuation is calibrated in two ways and is periodically checked for reproducibility.

Gain curves (microwave power as a function of wiggler magnetic field) for a 1-, 2-, and 3-meter long wiggler are shown in Fig. 3. The peak of the gain curve shifts from 3.8 kG for a 1-meter long wiggler to 3.6 kG for the 2- and 3-meter long wiggler. Also, the 2- and 3-meter gain curves show an asymmetric plateau on the long wavelength side of the curve. Both these phenomena (shifted gain curve peak and asymmetric gain curve) are indicative of saturation. In all cases, the full width of the gain curve at the 3 dB points is about 10% ($\Delta f_{3dB}/f_{res}$).

Using a resonant field of 3.8 kG (corresponding to the peak of the gain curve for the unsaturated amplifier) we studied the amplifier performance as a function of its length. The beam current through the wiggler is 850 Amps. The results of this experiment are shown in Fig. 4. The exponential growth region of this curve shows a gain of 34 dB/m. This is somewhat larger than

the 27 dB/m measured in the small signal gain experiment. The amplifier saturates at a wiggler length of 1.4 meters with 150 MW output power in the TE_{01} mode.

Beyond saturation, the output power oscillates with a period of about 1 meter. This oscillation is a manifestation of the synchrotron motion of the trapped electrons in the ponderomotive well.⁶ The measured synchrotron period is slightly larger than the synchrotron period given by

$$\lambda_{\text{synch}} = 2\pi \left[\frac{\gamma_r^2 m^2 c^3}{e^2 E_s B_w} \right]^{1/2} \quad (\text{MKS}) \quad (1)$$

where E_s is the peak electric field of the radiation. This calculated value is 0.8 m. At least part of the discrepancy can be attributed to the space charge forces of the electron beam.⁷

When the exponential gain portion of the curve is extrapolated back to the origin, the signal at the input to the wiggler is 5 kW, which is 10% of the injected power from the magnetron. This apparent discrepancy can be explained in terms of injection losses.⁸ The electric field of the input signal can couple into three modes of the FEL: one mode decays, one mode oscillates, and the third amplifies. Thus, only one third of the input electric field, or one ninth of the input power, actually gets amplified.

MODES

Since the radiation of the FEL is confined to a waveguide, the FEL resonance condition must satisfy the dispersion relation of the waveguide ($\omega_s^2 = k_s^2 c^2 + \omega_{co}^2$, where ω_{co} is the cutoff frequency for a particular mode in the waveguide). The resonant energy for the FEL interaction is

$$\gamma_{\text{res}}^2 = \frac{1}{2} \left[\frac{\omega_s/c}{k_w + (k_s - \omega_s/c)} \right] (1 + a_w^2) \quad (2)$$

where $a_w^2 = \frac{1}{2} \left[\frac{eB_w \lambda_w}{mc \cdot 2\pi} \right]^2$. For a well-matched beam (no transverse betatron motion) only the TE_{m1} ($m > 0$) modes with an even number m contribute, since these modes have power on axis with the correct polarization. The resonant energy (in terms of the resonant energy for the fundamental) for the first few higher order modes is listed in Table 1. The TE_{21} (TM_{21}) mode is sufficiently close in resonant energy to the fundamental that we are concerned with energy transfer into this mode.

TABLE 1.

Mode	$\gamma_{\text{res}}(m,1)/\gamma_{\text{res}}(0,1)$
TE_{01}	1
TE_{21} (TM_{21})	1.02
TE_{41} (TM_{41})	1.11

In order to measure the energy in the TE_{21} and TM_{21} modes, we placed an array of detectors in the far field of the radiation pattern to measure the peak signal in each mode. In the far field, a minimum in the fundamental is near the maximum in the TE_{21} or TM_{21} radiation pattern. This is illustrated in Fig. 5. The angle θ is in the plane defined by the electric field of the radiation and the axis of the waveguide. ϕ is the angle of rotation of this plane about the waveguide axis. Fig. 6 shows the radiation patterns for the TE_{01} and TE_{21} (TM_{21}) modes in the $\phi = 0$ plane. The location of the mode

detector is indicated in this figure. To distinguish between the TE_{21} and TM_{21} modes, detectors with different polarizations were placed in the far field at $\phi = 45^\circ$ and $\theta = 12^\circ$. At that point, the E-fields from the TE_{21} and TM_{21} modes are orthogonal.

Fig. 6 shows the total power output ($TE_{01} + TE_{21} + TM_{21}$) as a function of wiggler length. The power in TE_{01} mode only is also shown; the difference between the two curves is the power in the TE_{21} and TM_{21} modes. We found that the power in the (2,1) modes is equally divided between the TE_{21} and TM_{21} modes which is consistent with their being degenerate modes.⁹ Fig. 7 shows the fraction of power residing in the particular modes as a function of wiggler length. The power in the fundamental and higher order modes is oscillating back and forth with a period about twice as long as the synchrotron period. This energy exchange is due to the overlapping buckets of the TE_{01} and TE_{21} (TM_{21}) modes.

HARMONICS

In a linearly polarized wiggler, the electron orbits exhibit longitudinal oscillations along the axis of the wiggler.¹⁰ These oscillations result in radiation at odd harmonics of the fundamental. It should be pointed out that the electrons are not resonant with the third harmonic; therefore, there is no FEL gain at this frequency. Estimates for third harmonic output power indicate that about 1% of the power at the fundamental might be generated at the third harmonic.¹¹

A detector was placed on axis to monitor the third harmonic radiation. Fig. 8 shows power on axis (TE_{01}) for the fundamental frequency as well as the

third harmonic. The peak output power was slightly reduced (~100 MW). There was about 200 kW to 300 kW in the third harmonic. In addition, the third harmonic power as a function of wiggler length exhibits a structure corresponding to the synchrotron motion of the trapped electrons. In this experiment, the synchrotron period is 1.2 meters, even though the peak power appears to be reduced.

SUMMARY

A Free Electron Laser Amplifier has operated at 35 GHz with a peak output power of 180 MW, with a 3 MeV, 850 A electron beam. This corresponds to an extraction efficiency of 7%. The FEL has an operating bandwidth of approximately 10%, based on gain curve measurements. The amplifier saturates at a wiggler length of 1.4 meters. Beyond saturation the output power oscillates due to the synchrotron motion of the trapped electrons in the ponderomotive well. The synchrotron period is about 1.1 m. Power in the TE_{21} , and TM_{21} modes is appreciable (~50% of the total power) competing for resonance with the fundamental mode. The power radiated at the third harmonic is a few percent of the peak fundamental power ($P_{3\omega} \sim 200$ kW).

ACKNOWLEDGEMENTS

We would like to thank Dr. John Clark and the ETA staff for their valuable assistance in operating the ETA. We also wish to acknowledge Dr. Frank Chambers for the data acquisition routines which greatly facilitated the collection and analysis of the data.

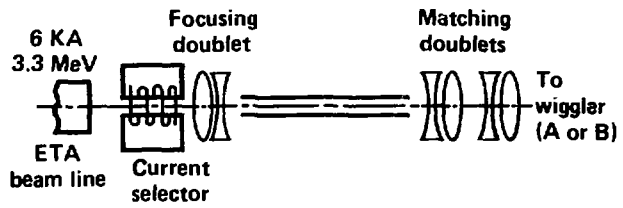
FIGURE CAPTIONS

- Fig. 1. Schematic of the Electron Laser Facility. Configuration A illustrates the method for measuring the small signal gain. Configuration B shows the amplifier mode of operation.
- Fig. 2. Small signal gain in the super-radiant mode as a function of wiggler length. Extrapolating the signal back to the origin gives an effective input signal of 1.3 mW.
- Fig. 3. Amplified microwave power output as a function of wiggler magnetic field for a 1-, 2-, and 3-meter long wiggler. The amplifier saturates at 1.4 m.
- Fig. 4. Amplified microwave power output as a function of wiggler length for constant wiggler field ($B_w = 3.8$ kG) corresponding to the peak of the gain curve before saturation.
- Fig. 5. Far field radiation patterns for the TE_{01} and TE_{21} (TM_{21}) modes in the plane defined by the electron wiggle motion ($\phi = 0$). A microwave detector is located at the position shown to monitor the higher order modes.
- Fig. 6. Amplified microwave power as a function of wiggler length for a fixed wiggler magnetic field ($B_w = 3.8$ kG). The two curves correspond to the total power, $TE_{01} + TE_{21} + TM_{21}$, (\bullet), and to the power in the fundamental mode, TE_{01} , (\blacktriangle).
- Fig. 7. Fraction of total power in the TE_{01} mode and in the TE_{21} and TM_{21} modes as a function of wiggler length.
- Fig. 8. Amplified microwave power as a function of wiggler length showing the radiated power in the fundamental frequency, 35 GHz, and at the third harmonic, 105 GHz. Both signals were measured in the far field along the wiggler axis and correspond to the TE_{01} mode.

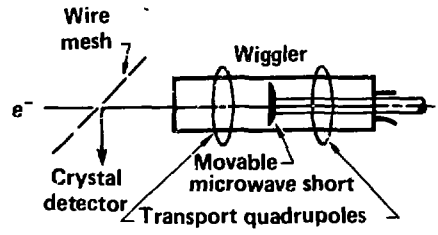
REFERENCES

1. T. J. Orzechowski, E. T. Scharlemann, B. R. Anderson, V. K. Neil, W. M. Fawley, D. Prosnitz, S. M. Yarema, D. B. Hopkins, A. C. Paul, A. M. Sessler, and J. S. Wurtele, "High-Gain Free Electron Lasers Using Induction Linear Accelerators," IEEE J. Quantum Electron., vol. QE-21, pp.831-844, 1985, and references therein.
2. J. T. Weir, G. J. Caporaso, F. W. Chambers, R. Kalibjian, J. Kallman, D. S. Prono, M. E. Slominski, A. C. Paul, "Improved Brightness of the Advanced Test Accelerator Injector," paper T15; 1985 Particle Accelerator Conf., Vancouver, BC, May 13-16, 1985. Also Lawrence Livermore National Laboratory Report UCRL-91939, May 7, 1985.
3. A. C. Paul, A. M. Sessler, J. S. Wurtele, G. J. Caporaso, and A. G. Cole, "A Variable Emittance Filter for the Electron Laser Facility," in Free Electron Generators of Coherent Radiation, C. A. Brau, S. F. Jacobs, and M. O. Scully, Eds., Bellingham, WA: SPIE, 1983, pp. 108-113.
4. T. J. Orzechowski, B. R. Anderson, W. M. Fawley, D. Prosnitz, E. T. Scharlemann, D. B. Hopkins, A. C. Paul, A. M. Sessler, and J. S. Wurtele, "Microwave Radiation from a High-Gain Free Electron Laser Amplifier," Phys. Rev. Lett., vol. 54, pp. 889-892, 1985.
5. T. J. Orzechowski, M. C. Moebus, F. A. Penko, D. Prosnitz, D. Rogers, C. S. Chavis, K. Halbach, D. B. Hopkins, R. W. Kuenning, A. C. Paul, A. M. Sessler, G. D. Stover, J. T. Tanabe, R. M. Yamamoto, and J. S. Wurtele, "The Status of the Lawrence Berkeley Laboratory and Lawrence Livermore National Laboratory (LLNL) Free Electron Laser (FEL)," in Free Electron Generators of Coherent Radiation, C. A. Brau, S. F. Jacobs, and M. O. Scully, Eds., Bellingham, WA: SPIE, 1983, pp. 55-74.
6. N. M. Kroll, P. L. Morton, and M. R. Rosenbluth, "Free Electron Lasers with Variable Parameter Wigglers," IEEE J. Quantum Electron., vol. QE-17, pp. 1436-1468, 1981.
7. E. T. Scharlemann, W. M. Fawley, T. J. Orzechowski, "Comparison of the Livermore Microwave FEL Results at ELF with 2D Numerical Simulation," Proceedings of the 7th International Free Electron Conference, Tahoe City, CA, 8-13 September 1985.
8. P. Sprangle, private communication.
9. J. S. Wurtele, "Multiple Waveguide Mode Effects in Free Electron Lasers," Ph.D. thesis, University of California, Berkeley, 1985.
10. W. R. Colson, "Nonlinear Wave Equation for Higher Harmonics in Free Electron Lasers," IEEE J. Quantum Electron., vol. QE-17, pp. 1417-1426, 1981.
11. T. J. Karr, E. T. Scharlemann, private communication.

TJO/jc:0236c



Configuration A



Configuration B

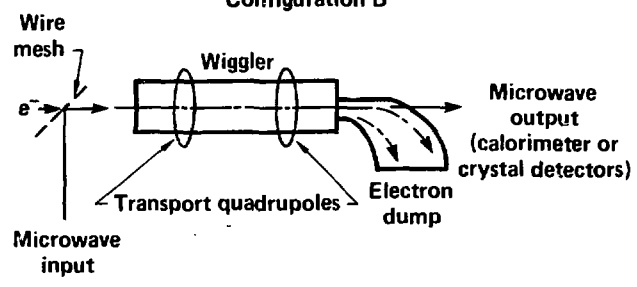


Fig. 1

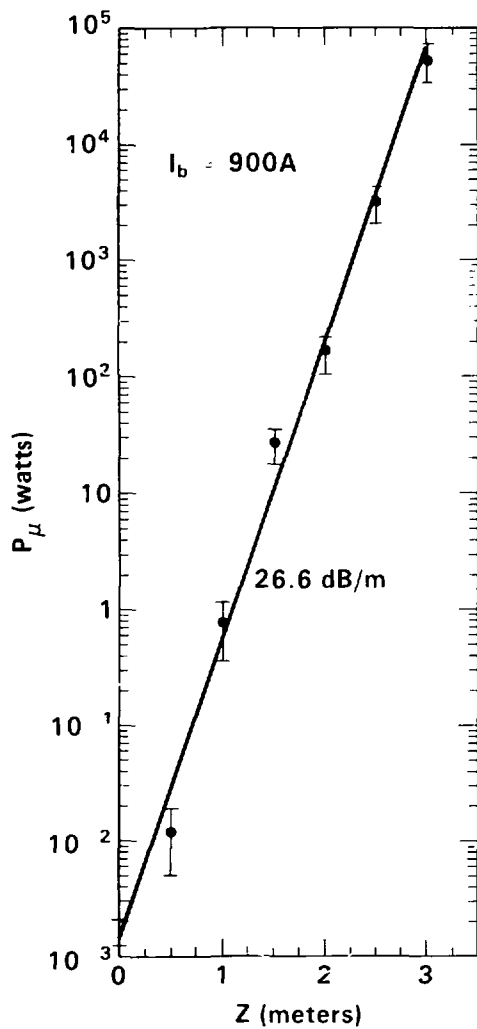


Fig. 2

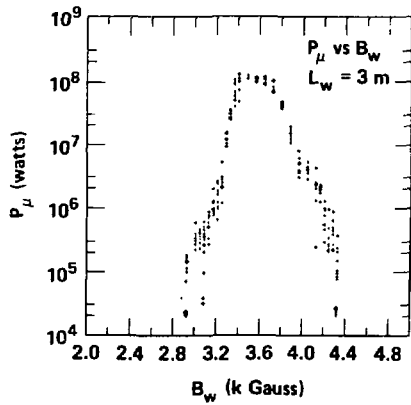
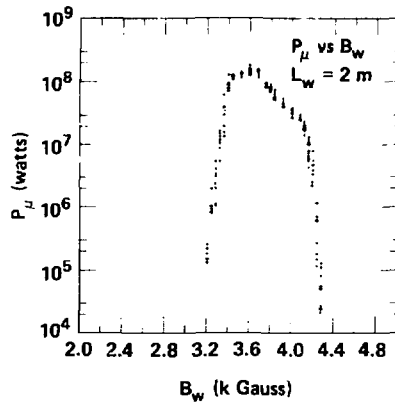
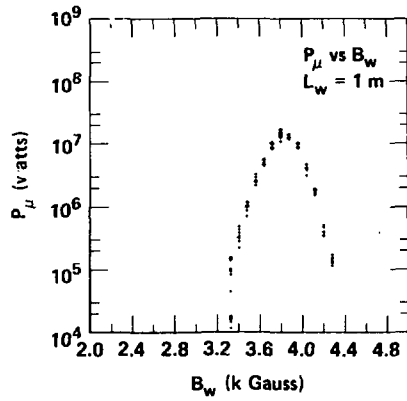


Fig. 3

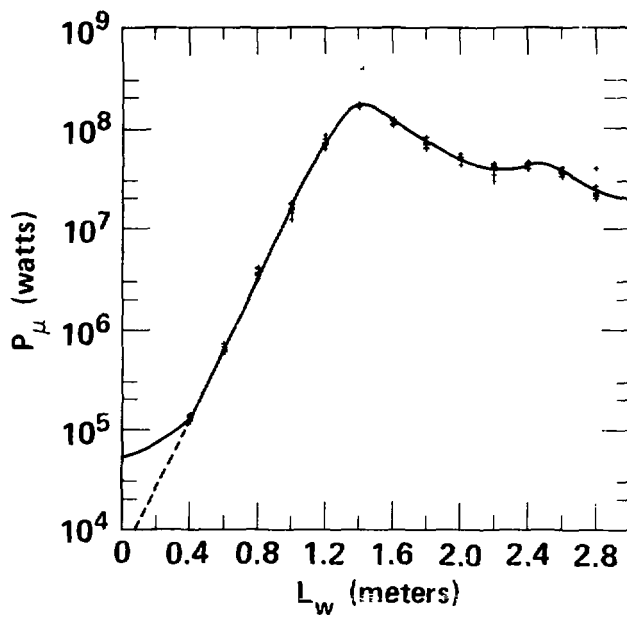


Fig. 4

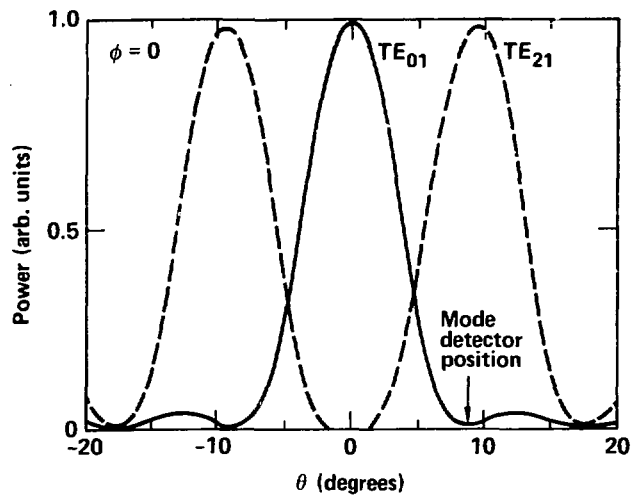


Fig. 5

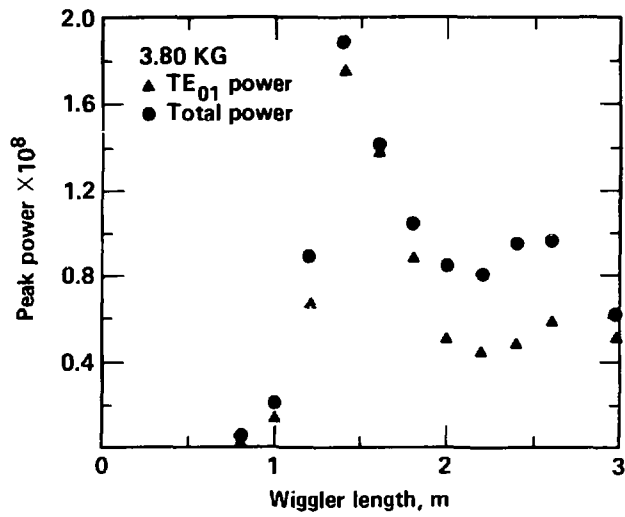


Fig. 6

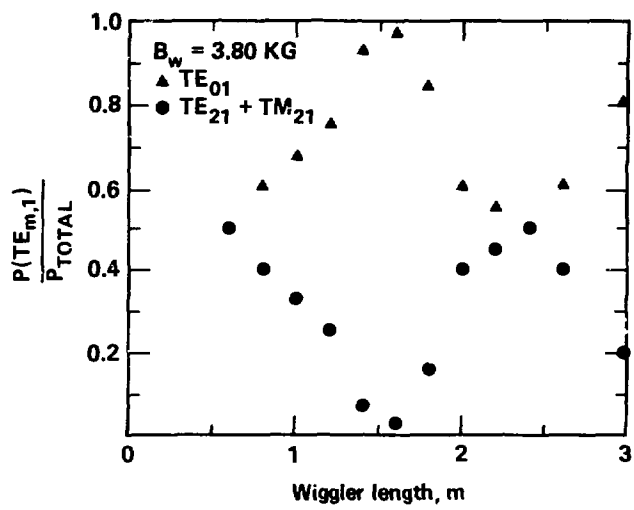


Fig. 7

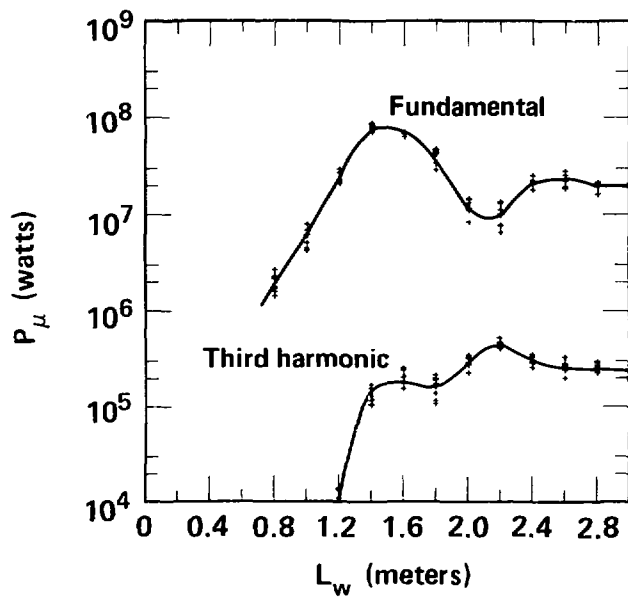


Fig. 8

DISCLAIMER

This report was prepared as an account of work sponsored by an agency of the United States Government. Neither the United States Government nor any agency thereof, nor any of their employees, makes any warranty, express or implied, or assumes any legal liability or responsibility for the accuracy, completeness, or usefulness of any information, apparatus, product, or process disclosed, or represents that its use would not infringe privately owned rights. Reference herein to any specific commercial product, process, or service by trade name, trademark, manufacturer, or otherwise does not necessarily constitute or imply its endorsement, recommendation, or favoring by the United States Government or any agency thereof. The views and opinions of authors expressed herein do not necessarily state or reflect those of the United States Government or any agency thereof.